Inorg. Chem. **2004**, *43*, 5096–5102

Synthesis, Crystal Structure, and Luminescent Properties of a Binuclear Gallium Complex with Mixed Ligands

Juan Qiao, Li D. Wang, Lian Duan, Yang Li, De Q. Zhang, and Yong Qiu*

Key Lab of Organic Optoelectronics & Molecular Engineering of Ministry of Education, Beijing 100084, China, and the Department of Chemistry, Tsinghua University, Beijing 100084, China

Received March 24, 2004

By introducing tridentate Schiff base ligands, a binuclear gallium complex with mixed ligands, bis(salicylidene-*o*-aminophenolato)-bis(8-quinolinolato)-bis-gallium(III) [$Ga_2(saph)_2q_2$], has been synthesized and structurally characterized by single-crystal X-ray crystallography. Crystal data for $C_{44}H_{30}Ga_2N_4O_6$ are as follows: space group, triclinic, $P\bar{1}$; $a = 11.357(3)$ Å, $b = 12.945(3)$ Å, $c = 12.947(3)$ Å, $\alpha = 103.461(15)°$, $\beta = 100.070(7)°$, $\gamma = 96.107(18)°$, $Z = 2$. This complex was identified as a dimeric complex of hexacoordinated gallium with strong intermolecular and intramolecular π–π stacking interactions between the pyridyl/pyridyl rings. The thermal analysis showed that $Ga_2(saph)_2q_2$ can readily form a stable amorphous glass with a high glass transition temperature ($T_g = 204$ °C), which is 27 °C higher than that of tris(8-hydroxyquinolinolate)aluminum (Alq_3). In addition, a high photoluminescence efficiency (ϕ_{PL}) of 0.318 in DMF has been demonstrated, although the central gallium atom can result in heavy-atom quenching. Organic light-emitting diodes (OLEDs) based on this complex displayed a turn-on voltage as low as 2.5 V and a high efficiency. Even at a low doping concentration of 1%, the doped $Ga_2(saph)_2q_2$ devices with 4-(dicyanomethylene)-2-*tert*-butyl-6-(1,1,7,7-tetramethyljulolidyl-9-enyl)-4*H*-pyran (DCJTB) as the dopant exhibited excellent red emission centered at 628 nm with improved durability, compared with the case of Alq_3 as the host. These distinguishing properties of $Ga_2(saph)_2q_2$ make it a good candidate as a novel electron-transporting and emitting material for OLEDs.

Introduction

Since the first report of organic light-emitting diodes (OLEDs) fabricated from tris(8-hydroxyquinolinolate)aluminum(III) (Alq_3) in 1987,[1] organic metal chelate complexes have attracted much attention due to their high thermal stability, adequate electron transport, and luminescent properties.[2] Alq_3 is a stable metal chelate complex that can be sublimed to yield amorphous thin films and stands as the most widely used electron-transport host or emitting material for OLEDs.[3,4] However, Alq_3 itself has relatively low photoluminescence (PL) quantum yield and electron mobility.[5,6] In addition, many derivatives of Alq_3 have been investigated as emitter materials, including those with substitution of the metal ion with other trivalent metals[7,8] and substitution of the 8-quinolinol ligand.[9−11] In recent years, the most promising candidates to substitute Alq_3 were thought to be complexes with gallium as the central atom.[7,12] Forrest and coworkers have reported that devices made from Gaq_3 and Alq_3 have similar electroluminescence (EL) quantum efficiencies, while the Gaq_3 devices exhibit a lower turn-on voltage and hence a proportionately higher power efficiency than the Alq_3 devices by 50%.[7] Sapochak et al.[13] presented a series of bis(8-hydroxyquinaldine)gallium(III) complexes (i.e., q_2GaX,

* To whom correspondence should be addressed. E-mail: qiuy@mail.tsinghua.edu.cn. Phone: (008610) 62788802. Fax: (008610) 62795137.

(1) Tang, C. W.; VanSlyke, S. A. *Appl. Phys. Lett.* **1987**, *51*, 913.
(2) Chen, C. H.; Shi, J. M. *Coord. Chem. Rev.* **1998**, *171*, 161.
(3) Brinkmann, M.; Gadret, G.; Muccini, M.; Taliani, C.; Masciocchi, N.; Sironi, A. *J. Am. Chem. Soc.* **2000**, *122*, 5147.
(4) Hung, L. S.; Chen, C. H. *Mater. Sci. Eng., R* **2002**, *39*, 143.
(5) Tang, C. W.; VanSlyke, S. A.; Chen, C. H. *J. Appl. Phys.* **1989**, *65*, 3610.
(6) Hosokawa, C.; Tokailin, H.; Higashi, H.; Kusumoto, T. *Appl. Phys. Lett.* **1992**, *60*, 1220.
(7) Burrows, P. E.; Sapochak, L. S.; McCaty, D. M.; Forrest, S. R.; Thompson, M. E. *Appl. Phys. Lett.* **1994**, *64*, 2718.
(8) Chen, B. J.; Sun, X. W.; Li, Y. K. *Appl. Phys. Lett.* **2003**, *82*, 3017.
(9) Sapochak, L. S.; Padmaperuma, A.; Washton, N.; Endrino, F.; Schmett, G. T.; Marshall, J.; Fogarty, D.; Burrows, P. E.; Forrest, S. R. *J. Am. Chem. Soc.* **2001**, *123*, 6300.
(10) Kido, J.; Lizumi, Y. *Appl. Phys. Lett.* **1998**, *73*, 2721.
(11) Leung, L. M.; Lo, W. Y.; So, S. K.; Lee, K. M.; Choi, W. K. *J. Am. Chem. Soc.* **2000**, *122*, 5640.
(12) Elschener, A.; Heuer, H. W.; Jonas, F.; Kirchmeyer, S.; Wehrmann, R.; Wussow, K. *Adv. Mater. (Weinheim, Ger.)* **2001**, *13*, 1811.

10.1021/ic049603s CCC: $27.50
Published on Web 07/09/2004

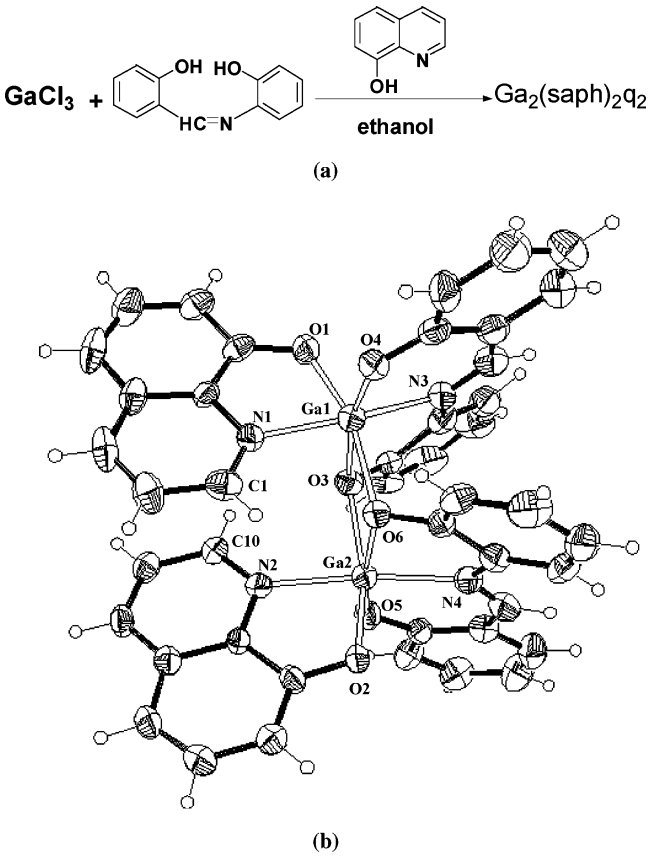

Figure 1. (a) Synthetic scheme of $Ga_2(saph)_2q_2$; (b) ORTEP plot of $Ga_2(saph)_2q_2$ with 35% probability ellipsoids, showing the main complexing atomic numbering scheme.

with X = acetate, dimethylpropionate, benzoate, and chloro). Elschner et al.[12] reported an oxo-bridged gallium complex, $2(Gaq_2)O$, which could be deposited from methanol solution. These Ga complexes are all pentacoordinate, in which Ga^{3+} ions coordinate bidentate and monodentate ligands, and show blue-shifted light relative to the hexacoordinate Alq_3.

Our group has focused on metal(III) complexes based on tridentate Schiff base ligands, which have also proven to be highly efficient luminescent materials for OLEDs.[14,15] By introducing a tridentate Schiff base ligand, a novel gallium complex (Figure 1), bis(salicylidene-*o*-aminophenolato)-bis-(8-quinolinolato)-bis-gallium(III) [$Ga_2(saph)_2q_2$], has been synthesized and structurally characterized as a dimeric complex of hexacoordinated gallium, and it has been shown to be of high luminescent efficiency. By using this complex as the host material, pure red OLEDs have been reported with higher efficiency than the doped Alq_3 devices.[14] The large improvement is due not only to the excellent energy match of the host−guest system but also to the inherent properties of $Ga_2(saph)_2q_2$. Herein, we report the synthesis, crystal structure, PL, and EL of this novel dimeric complex. The results are compared with tris(8-hydroxyquinolinolate) complexes of Al and Ga (Alq_3 and Gaq_3).

Experimental Section

Materials. $GaCl_3$ (99.99%) was used as purchased from Aldrich Chemical Co. The tridentate ligand of salicylidene-*o*-aminophenol (saph) was obtained by heating the mixture of salicylaldehyde and *o*-hydroxyaniline in a 1:1 molar ratio, and the resultant product was recrystallized in ethanol.

Synthesis of $Ga_2(saph)_2q_2$. $Ga_2(saph)_2q_2$ was prepared through a reaction in ethanol solution of $GaCl_3$, q (8-hydroxyquinoline), and saph (salicylidene-*o*-aminophenol), as shown in Figure 1. First, a solution of saph (1.065 g, 5 mmol) and piperidine (1.0 mL,10 mmol) in ethanol (50 mL) was slowly added to a solution of $GaCl_3$ (0.88 g, 5 mmol) in 10 mL of ethanol. After the mixture had stirred for 0.5 h, a solution of q (0.72 g, 5 mmol) and piperidine (0.5 mL, 5 mmol) in ethanol (10 mL) was introduced, the mixture was stirred for about 2 h, and a yellow precipitate was produced. The crude product was collected by filtration, washed with ethanol rapidly, and finally dried under an infrared lamp. The material was further purified by gradient-temperature sublimation (twice) before analysis and device fabrication. Yield: 80%. MS (EI) [*m*/*z*]: 851, 850, 705, 538, 495, 493, 425, 213, 145. Anal. Calcd for $C_{22}H_{15}N_2O_3Ga$: C, 62.12; H, 3.53; N, 6.59; O, 11.29. Found: C, 62.26; H, 3.52; N, 6.52; O, 11.53. ^{1}H NMR (DMSO-d_6, 400 MHz), ppm: 9.23 (s, 2H), 8.45 (d, J = 8 Hz, 2H), 7.78 (d, J = 8 Hz, 2H), 7.52−7.48 (m, 8H), 7.19−7.15 (m, 2H), 7.12 (d, J = 8 Hz, 2H), 6.96 (t, J = 7 Hz, 2H), 6.85 (d, 2H), 6.63 (t, J = 7 Hz, 2H), 6.58 (t, J = 7 Hz, 2H), 6.45 (d, J = 8 Hz, 4H). IR (cm^{-1}): 3063, 1617, 1603, 1578, 1541, 1499, 1467, 1446, 1383, 1332, 1317, 1284, 1263, 1240, 1226, 1177, 1151, 1119, 1056, 1034, 925, 842, 823, 787, 747.

X-ray Crystallography. A single crystal suitable for X-ray crystallography was isolated by gradient-temperature vacuum sublimation. $Ga_2(saph)_2q_2$ was heated incrementally in zone 1 of a two-zone furnace from 270 to 320 °C under a nitrogen atmosphere with a base pressure of 2 Pa for 12 h. The single crystal was collected at 300 °C and has a typical size of 0.1 × 0.2 × 0.2 mm^3. The solid-state structure was further confirmed by single-crystal X-ray diffraction analysis. The room temperature (294 ± 1 K) single-crystal X-ray experiments were performed on a Bruker P4 diffractometer equipped with graphite-monochromatized Mo Kα radiation (λ = 0.710 73 Å). The 2θ range is 6.6−22.4°. Direct phase determination yielded the positions of Ga, O, N, and most of the C atoms. The remaining atoms were located in successive-difference Fourier syntheses. Hydrogen atoms were generated theoretically and rode on their parent atoms in the final refinement. All non-hydrogen atoms were subjected to anisotropic refinement. The structural solutions and refinements were performed using the SHELXTL NT v 5.10 program package (Bruker, 1997).[16] A summary of the refinement details and the resulting factors is given in Table 1.

Equipment. Elemental analysis was carried out on an Elementar Vario EL (Germany) elemental analyzer. ^{1}H NMR spectra were recorded on a Bruker ARX400 NMR spectrometer with tetramethylsilane as the internal standard. Infrared spectra were recorded on a Nicolet Magna-IR 750 FT-IR microscope system. Absorption spectra were recorded with a UV−vis spectrophotometer (HITACHI U3010), and PL spectra were obtained with a fluorospectrophotometer (HITACHI, F4500). Relative PL quantum efficiencies (ϕ_{PL}) were determined from degassed dimethyl formamide (DMF) solutions, and the concentrations of the samples were carefully

(13) Sapochak, L. S.; Burrows, P. E.; Garbuzov, D.; Ho, D. M.; Forrest, S. R.; Thompson, M. E. *J. Phys. Chem.* **1996**, *100*, 17766.
(14) Qiao, J.; Qiu, Y.; Wang, L. D.; Duan, L.; Li, Y.; Zhang, D. Q. *Appl. Phys. Lett.* **2002**, *81*, 4913.
(15) Shao, Y.; Qiu, Y.; Hu, W. H.; Hong, X. Y. *Adv. Mater. Opt. Electron.* **2000**, *10*, 285.
(16) Sheldrick, G. M. *SHELXTL*, version 5.1; Bruker Analytical X-ray System, Inc.: Madison, WI, 1997.

Table 1. Crystallographic Data

formula	$C_{44}H_{30}Ga_2N_4O_6$
fw	850.16
color	yellow prism
cryst size, mm^3	0.1 × 0.2 × 0.2
cryst syst	triclinic
space group	$P\bar{1}$ (No. 2)
a, Å	11.357(3)
b, Å	12.945(3)
c, Å	12.947(3)
α, deg	103.461(15)
β, deg	100.070(7)
γ, deg	96.107(18)
V, Å^3	1801.1(7)
Z	2
d_{calcd}, g cm^{-3}	1.568
μ, cm^{-1}	1.554
$2\theta_{max}$, deg	50
F(000)	864
reflns measured	6655/6281
R_{int}	0.05
GOF on F^2	1.068
R1, wR2 [$I \geq 2\sigma(I)$][a]	0.1012, 0.0627
R1, wR2 (all data)[a]	0.1502, 0.1290

[a] $R1 = \sum|F_o| - |F_c|/\sum|F_o|$; $wR2 = [\sum w(F_o^2 - F_c^2)^2/\sum w(F_o^2)^2]^{1/2}$.

Table 2. Selected Bond Lengths (Å) and Angles (deg)

Ga(1)−O(4)	1.895(5)	Ga(2)−O(5)	1.898(5)
Ga(1)−O(1)	1.934(4)	Ga(2)−O(2)	1.944(4)
Ga(1)−N(3)	2.029(6)	Ga(2)−O(6)	2.049(5)
Ga(1)−O(6)	2.044(4)	Ga(2)−N(4)	2.050(6)
Ga(1)−N(1)	2.064(5)	Ga(2)−N(2)	2.084(5)
Ga(1)−O(3)	2.072(4)	Ga(2)−O(3)	2.053(4)
O(4)−Ga(1)−O(1)	100.6(2)	O(5)−Ga(2)−O(2)	102.3(2)
O(4)−Ga(1)−N(3)	92.7(2)	O(5)−Ga(2)−O(6)	164.2(2)
O(1)−Ga(1)−N(3)	91.7(2)	O(2)−Ga(2)−O(6)	90.04(18)
O(4)−Ga(1)−O(6)	94.79(19)	O(5)−Ga(2)−N(4)	92.5(2)
O(1)−Ga(1)−O(6)	160.96(19)	O(2)−Ga(2)−N(4)	89.0(2)
O(6)−Ga(1)−O(3)	76.10(17)	O(6)−Ga(2)−N(4)	79.4(2)
N(3)−Ga(1)−O(3)	80.0(2)	O(5)−Ga(2)−O(3)	93.46(19)
N(1)−Ga(1)−O(3)	96.8(2)	O(2)−Ga(2)−O(3)	160.24(18)
O(4)−Ga(1)−N(1)	91.6(2)	O(6)−Ga(2)−O(3)	76.39(17)
O(1)−Ga(1)−N(1)	82.3(2)	N(4)−Ga(2)−O(3)	102.2(2)
N(3)−Ga(1)−N(1)	173.2(2)	O(5)−Ga(2)−N(2)	91.1(2)
O(6)−Ga(1)−N(1)	86.1(2)	O(2)−Ga(2)−N(2)	81.8(2)
O(4)−Ga(1)−O(3)	167.13(19)	O(6)−Ga(2)−N(2)	98.85(19)
O(1)−Ga(1)−O(3)	90.27(18)	N(4)−Ga(2)−N(2)	170.7(2)
N(3)−Ga(1)−O(6)	98.8(2)	O(3)−Ga(2)−N(2)	86.2(2)
Ga(1)−O(6)−Ga(2)	104.1(2)	Ga(2)−O(3)−Ga(1)	103.0(2)

adjusted so that the optical densities at 390 nm (excitation wavelength) were <0.1 absorption units. PL quantum yields were finally calculated relative to the known value of Alq_3 in DMF ($\phi_{PL} = 0.116$)[17] and normalized to Alq_3. The equation

$$\Phi_s = \Phi_r\left(\frac{\eta_S^2 A_r I_s}{\eta_r^2 A_s I_r}\right)$$

was used to calculate quantum yields where Φ_s is the quantum yield of the sample, Φ_r is the quantum yield of the reference, η is the refractive index of the solvent, A_s and A_r are the absorbances of the sample and the reference at the wavelength of excitation, respectively, and I_s and I_r are the integrated areas of emission bands of the sample and the reference, respectively.[18]

Thermal analysis was determined by differential scanning calorimetry (DSC) performed on a TA thermal analysis instrument (DSC 2910 modulated DSC). A sample (5−10 mg) was placed in an aluminum pan and heated at a rate of 20 °C/min under N_2 gas flow at a rate of 50 mL/min. The melted samples were cooled rapidly and then heated a second time. Indium metal was used as the temperature standard. The glass transition temperature (T_g) and the crystallization point (T_{c1}) were determined through a second heating of the glassy state.

Fabrication of EL Devices. Devices were grown on glass slides that had been precoated with indium tin oxide (ITO) with 30 Ω/square. The substrates were ultrasonically cleaned in detergent solution for ∼1 min followed by thorough rinsing in deionized water. They were then rinsed in acetone followed by methanol and dried in pure nitrogen gas between each step. The organic films were deposited, layer by layer, onto the ITO surface. After deposition of the organic layers, a Mg/Ag (10:1 mass ratio) electrode was deposited onto the organic layer without breaking the vacuum. The chamber pressure was below 5×10^{-4} Pa during deposition of the organic materials and the metals. The doping process was carried out by the coevaporation method. The active area of the devices is 0.35 cm^2. Devices were tested in air with ITO as the positive electrode in the forward bias configuration without further encapsulation. Current−voltage luminance ($I-V-L$) of OLEDs was measured using a Keithley 4200 semiconductor characterization system. The EL spectra and Commission Internationale de l'Eclairage (CIE) color coordinates were measured with a Photo Research PR650 spectrophotometer.

Results and Discussion

Dimeric Structure and Crystal Packing. The molecular structure of the gallium complex has been elucidated by X-ray crystallography. The crystal data and selected bond lengths and angles are listed in Tables 1 and 2, respectively. A perspective drawing of the structure is shown in Figure 1. Each gallium atom is hexacoordinate with two nitrogen and four oxygen atoms, and the angles around gallium approximate an octahedral orientation ranging from 76.10(17)° (O(6)−Ga(1)−O(3)) to 100.6(2)° (O(4)−Ga(1)−O(1)). Two Ga atoms are involved in bridging through the phenolato oxygen atom of *o*-hydroxyaniline. It is very interesting to find that the gallium and the bridging oxygen atoms form a rhombus cavity, in which the average side is 2.055 Å. The average Ga−O and Ga−N bond lengths of the q ligands in $Ga_2(saph)_2q_2$ are 1.939 and 2.074 Å, respectively, which is almost the same as that reported for Gaq_3.[19] The average Ga−N bond length of the saph ligands is 2.039 Å, which is slightly shorter than the Ga−N bond in Gaq_3.

As shown in Figure 2a, the two q ligands are approximately parallel, and the off-plane angle is only 10.7°. The two pyridyl/pyridyl rings of the q ligands exhibit an intramolecular $\pi-\pi$ stacking interaction of 3.31 Å, which occurs between atoms N(2) and C(1). Such an interaction is not possible in the Gaq_3 and may be of some importance when comparing the electroluminescent properties of these materials. An examination of the solid-state packing of $Ga_2(saph)_2q_2$ shows that there are close intermolecular $\pi-\pi$ stacking interactions between the pyridyl/pyridyl rings of the neighboring molecules. The stacking distance is 3.24 Å

(17) Lytle, F. E.; Storey, D. R.; Juricich, M. E. *Spectrochim. Acta, Part A* **1973**, *29A*, 1357.
(18) Brooks, J.; Babayan, Y.; Lamansky, S.; Djurovich, P. I.; Tsyba, I.; Bau, R.; Thompson, M. E. *Inorg. Chem.* **2002**, *41*, 3055.
(19) Schmidbaur, H.; Lattenbauer, J.; Dallas, L.; Muller, W. G.; Kumberger, O. *Z. Naturforsch., B: Chem. Sci.* **1991**, *46B*, 901.

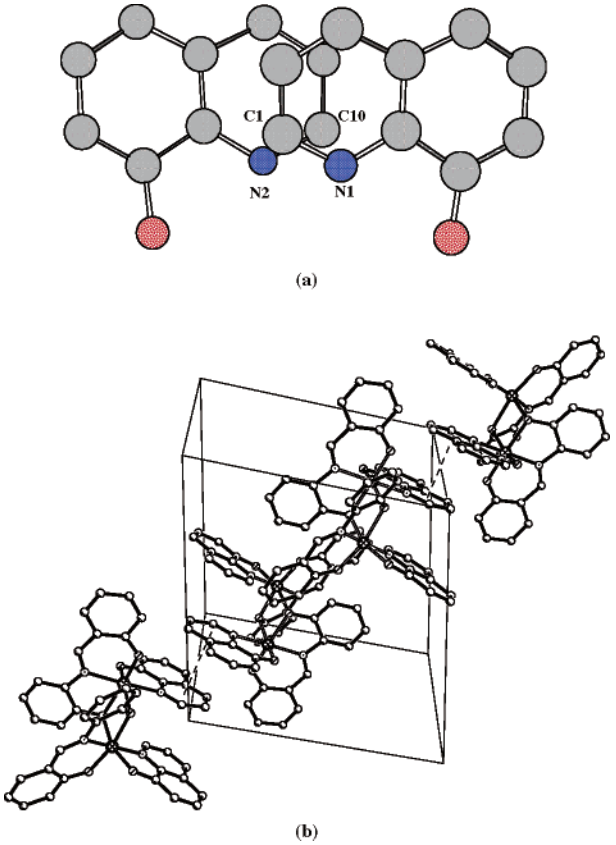

Figure 2. (a) Intramolecular interactions between the two q ligands; (b) intermolecular $\pi-\pi$ stacking (indicated by - - -) in $Ga_2(saph)_2q_2$.

(Figure 2b), which is shorter than the 3.35 Å between layers of graphite and the 3.4 Å between stacked nucleotide residues in DNA. Munakata et al.[20] argued that strong intermolecular interactions as well as intermolecular aromatic stacking could assist charge transfer. Recently, a binuclear aluminum 8-hydroxyquinoline complex ($DAlq_3$) was reported to exhibit higher electron mobility and higher EL efficiency than Alq_3.[21] It was suggested that the binuclear structure could increase the order of the molecule, thereby favoring high mobility. In organic molecules, charge transport is generally considered to be a disordered hopping process.[22] Charge carrier mobilities in these disordered organic systems are dominated by the rate of charge transport between neighboring hopping sites. For Gaq_3, electron transport is the hopping from a Gaq_3 molecule to another Gaq_3 molecule, and the hopping is solely intermolecular. For $Ga_2(saph)_2q_2$, besides the intermolecular hopping, intramolecular hopping from a q ligand to another q ligand is suggested.

Thermal Stability. The durability, i.e., the thermal and morphological stability of deposited films, is another important factor that has dramatic influence on the physical performance of OLEDs. Usually, an amorphous film with higher glass transition temperature (T_g) is desired.[23] Therefore, DSC experiments were carried out to investigate the glass-forming properties and the phase transition of $Ga_2(saph)_2q_2$. Results are presented in Table 3. A second heating cycle of $Ga_2(saph)_2q_2$ revealed a high T_g at 204 °C and a broad recrystallization exotherm (T_{c1}) at ~290 °C. The reported T_g and T_{c1} for Alq_3 are 177 and 251 °C, respectively, giving differences of 27 and 39 °C, respectively. Gaq_3 was reported to have a much lower T_{c1} value, by 46 °C.[9] To verify the amorphism of its films, thin films of $Ga_2(saph)_2q_2$ on quartz glass were prepared by vacuum deposition. As in the reference, thin films of Gaq_3 and Alq_3 were also prepared under the same conditions. The thicknesses of these films were all 50 nm. An atomic force microscope (AFM) was utilized to observe the morphology of the films on quartz glass. The image of the film surface morphology showed that the root-mean-square of the roughness was only about 0.6 nm in the case of $Ga_2(saph)_2q_2$, exhibiting better performance in film formation compared with Alq_3 and Gaq_3 (in Table 3). According to Shirota,[23] a nonplanar molecular structure can prevent easy packing of molecules and hence hinder crystallization. The glass transition temperature of molecular glasses can be increased by the incorporation of structurally rigid moieties and by increasing molecular size and weight, as well as by enhancing intermolecular interactions. The high T_g of $Ga_2(saph)_2q_2$ should be ascribed to the nonplanar binuclear molecular structure and the strong intermolecular interactions.

Table 3. Thermal Analysis and AFM Data

complex	T_g (°C)	T_{c1} onset (°C)	rms of AFM (nm)[b]
Alq_3	177[a]	251[a]	6.0
Gaq_3	n.o.[a]	244[a]	8.6
$Ga_2(saph)_2q_2$	204	290	0.6

[a] Referring to ref 9. [b] rms is the root-mean-square of the roughness.

Table 4. Photophysical Data in DMF Solution and Evaporated Film

	DMF solution				thin film	
complex	abs λ_{max} (nm)	emission λ_{max}[a] (nm)	Δ (cm^{-1})	relative ϕ_{PL} ($Alq_3 = 1.0$)	abs λ_{max} (nm)	emission λ_{max}[a] (nm)
Alq_3	388	518	6468	1.00	373	534
Gaq_3	392	540	6992	0.28	392	543
$Ga_2(saph)_2q_2$	441	540	4157	2.74	424	565

[a] $\lambda_{ex} = 390$ nm.

Photoluminescence. The room-temperature absorption and fluorescence spectra of $Ga_2(saph)_2q_2$ were measured both in dilute (~10^{-5} M) DMF solution and in film on a quartz substrate. The data are given Table 4 with Alq_3 and Gaq_3 used as the reference materials. Like Gaq_3, the optical transition of $Ga_2(saph)_2q_2$ is also centered on the organic ligands. As shown in Figure 3a, $Ga_2(saph)_2q_2$ exhibits a broad absorption band in the range 350−500 nm, which is remarkably different from that of the free q or saph.

To clarify how the two ligands contribute to the absorbance and emission of $Ga_2(saph)_2q_2$, we attempted to make the homoleptic dimer with saph. It was found that the mixture of saph ligand and metal salt showed desirable absorbance and emission in solutions, although no isolable homoleptic dimer was obtained. Such a mixture containing $Ga_2(saph)_3$

(20) Munakata, M.; Wu, L. P.; Kuroda-Sowa, T.; Maekawa, M.; Suenaga, Y.; Ning, G. L.; Kojima, T. *J. Am. Chem. Soc.* **1998**, *120*, 8610.
(21) Ma, D.; Wang, G.; Hu, Y.; Zhang, Y.; Wang, L.; Jing, X.; Wang, F.; Lee, C. S.; Lee, S. T. *Appl. Phys. Lett.* **2003**, *82*, 1296.
(22) Bässler, H. *Phys. Status Solidi B* **1993**, *175*, 15.
(23) Shirota, Y. *J. Mater. Chem.* **2000**, *10*, 1.

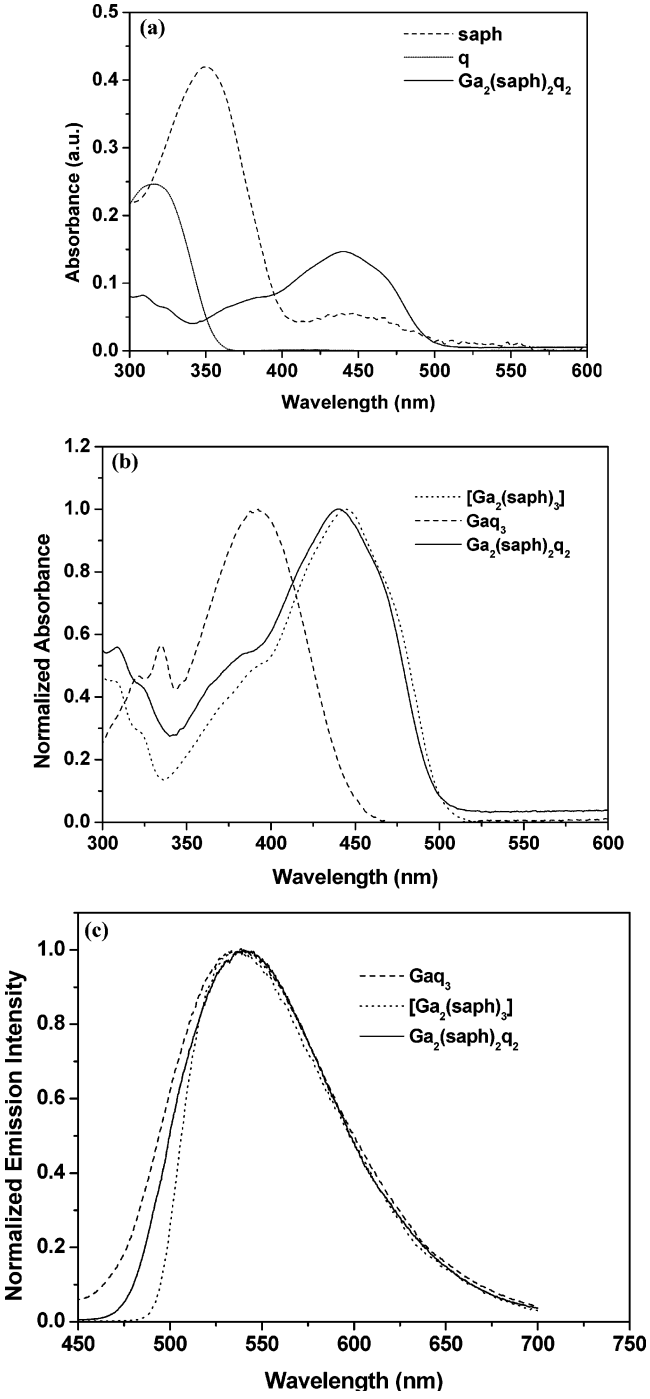

Figure 3. (a) UV−vis absorption spectra of saph, q, and $Ga_2(saph)_2q_2$ in DMF solutions; (b) UV−vis absorption spectra of $[Ga_2(saph)_3]$, Gaq_3, and $Ga_2(saph)_2q_2$ in DMF solutions; (c) normalized PL spectra of $[Ga_2(saph)_3]$, Gaq_3, and $Ga_2(saph)_2q_2$ in DMF solutions.

in DMF, as shown in Figure 3b,c, exhibits almost the same absorbance and emission as the mixed dimer of $Ga_2(saph)_2q_2$. Thus, it can be concluded that the absorbance and fluorescence of $Ga_2(saph)_2q_2$ arise mainly from metal-chelated saph ligands, not from the q ligand only. The lowest-energy absorption band centered at 440 nm should be assigned to the combination of the $\pi-\pi^*$ and $n-\pi^*$ transitions of the chelated saph, thus more intense than the $n-\pi^*$ transition of the free saph. Compared to the absorption of Gaq_3, a sizable red shift (about 50 nm) was observed in the

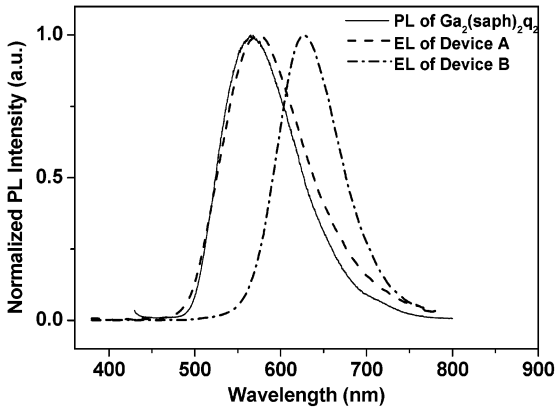

Figure 4. Normalized PL spectrum of the thin film of $Ga_2(saph)_2q_2$ and EL spectra of devices A and B.

absorption spectra of $Ga_2(saph)_2q_2$ due to the absorption of tridentate saph.

The Franck−Condon (F−C) shifts (Δ) indicate energy differences between absorption and emission maxima. A much smaller F−C shift was observed for $Ga_2(saph)_2q_2$ (4157 cm^{-1}) compared to that of Alq_3 (6393 cm^{-1}), which is presumably due to the rigid dimeric structure that hinders the geometrical relaxation. The PL quantum yields are investigated relative to the known quantum yield of Alq_3 in DMF. It is especially worthwhile to note that $Ga_2(saph)_2q_2$ shows very high PL efficiency (ϕ_{PL}) of 0.318 in DMF (2.74 times that of Alq_3), although the central gallium atom can result in heavy-atom quenching.[9] The heavy-atom effect determines the very low PL efficiency of Gaq_3 (approximately 4 times less than that of Alq_3). This exceedingly high PL efficiency should also be ascribed to the introduction of the tridentate ligands and the rigid dimeric structure, which is conducive to minimizing the nonradiative relaxation processes.

Electroluminescence. Finally, the emitting performance of $Ga_2(saph)_2q_2$ in OLEDs was investigated. Two types of devices were fabricated with $Ga_2(saph)_2q_2$ as an active layer. The type A device has a configuration of ITO (30 Ω)/NPB (40 nm)/$Ga_2(saph)_2q_2$ (40 nm)/Mg:Ag (A), where NPB is *N*,*N*′-biphenyl-*N*,*N*′-(1-naphthyl)-1,1′-biphenyl-4,4′-diamine, and was used as the hole-transporting material. $Ga_2(saph)_2q_2$ was used as the electron-transporting and emitting material. The type B device has a configuration of ITO (30 Ω)/NPB (60 nm)/$Ga_2(saph)_2q_2$:DCJTB (1%, 30 nm)/$Ga_2(saph)_2q_2$ (15 nm)/Mg:Ag (B), where $Ga_2(saph)_2q_2$ was used as the host and DCJTB [4-(dicyanomethylene)-2-*tert*-butyl-6(1,1,7,7,-tetramethyljulolidyl-9-enyl)-4*H*-pyran] was used as the dopant emitter. As the reference, an Alq_3-doped device was also fabricated with a configuration of ITO (30 Ω)/NPB (60 nm)/Alq_3:DCJTB (1%, 30 nm)/Alq_3 (15 nm)/Mg:Ag.

Figure 4 shows the PL spectrum of $Ga_2(saph)_2q_2$ and EL spectra of the two devices. The type A device exhibited bright orange light with the central wavelength of 576 nm, which comes from $Ga_2(saph)_2q_2$. Although the device is not optimized, the physical performance appears to be promising: turn-on voltage as low as 2.5 V (defined as the voltage required to give a brightness of 1 cd/m^2) and maximum

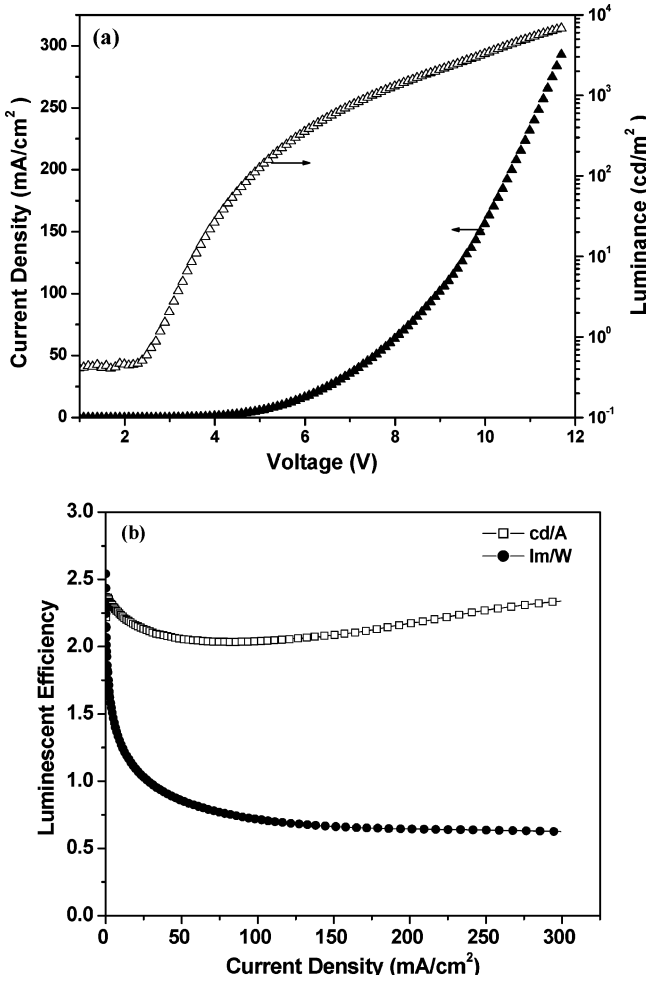

Figure 5. (a) Current density, voltage, and luminance characteristics; (b) luminescent efficiency vs current density for device B using $Ga_2(saph)_2q_2$ doped 1% DCJTB as the emitter.

power efficiency of 1.12 lm/W. In this case, $Ga_2(saph)_2q_2$ behaves as an excellent electron-injecting and -transporting material.

More recently, we reported a pure red OLED using $Ga_2(saph)_2q_2$ doped with 2% DCJTB, which showed a strong emission centered at 640 nm with two times higher efficiency than that of the doped Alq_3 device.[14] Here, we decreased the doping concentration of DCJTB to 1%; however, the $Ga_2(saph)_2q_2$-doped device (type B device) also gave excellent red emission with a peak wavelength of 628 nm. The full width at half-maximum is only 85 nm, and the color coordinates in the ′CIE 1931 chromaticity chart are $x = 0.633$ and $y = 0.364$. No light emission from $Ga_2(saph)_2q_2$ was measured, implying efficient energy transfer from $Ga_2(saph)_2q_2$ to DCJTB even at a low doping concentration of 1%. The device has a turn-on voltage as low as 2.5 V, a brightness of 7004 cd/m^2 at 11.7 V (Figure 5), and a luminous efficiency of 2.16 cd/A (1.09 lm/W) at 20 mA/cm^2 and 6.2 V. The doped Alq_3 device showed blue-shifted emission centered at 620 nm and CIE coordinates of (0.61, 0.38). As shown in Figure 6, there is an emitting peak of Alq_3 (520 nm) in addition to the red peak in this doping system. The device has a much lower brightness of 1500 cd/m^2 at 11.7 V.

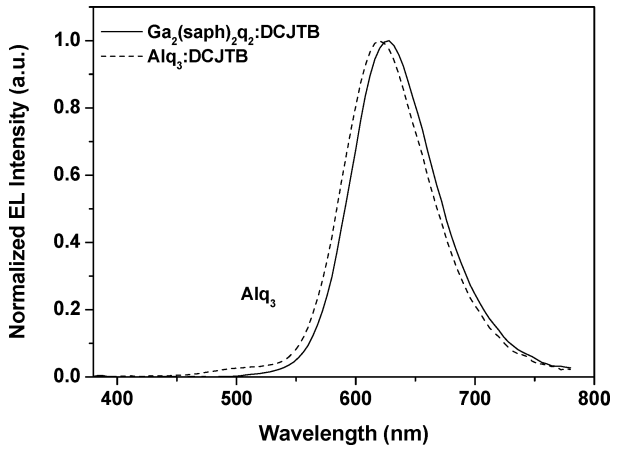

Figure 6. Normalized electroluminescent spectra of 1 wt % DCJTB doped devices.

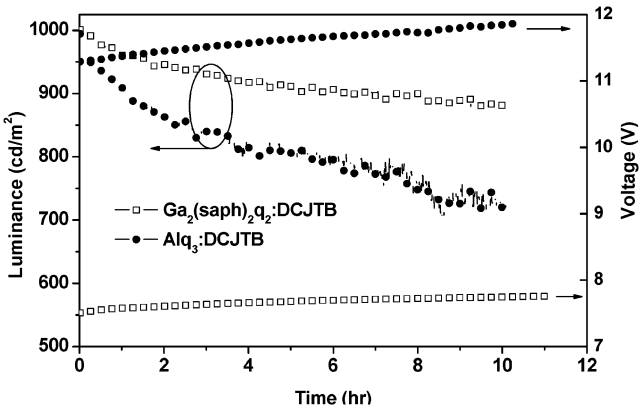

Figure 7. Plots of luminance decay and voltage increase as functions of operation time at room temperature for the DCJTB-doped OLEDs. The initial brightness was 1000 cd/m^2 under constant dc drive.

Through variation of the doping level of DCJTB from 1% to 3%, the $Ga_2(saph)_2q_2$-doped devices have shown great advantages over the Alq_3-doped devices with respect to maximum luminance, turn-on voltage, peak wavelength, and luminous efficiency, demonstrating the great potential of $Ga_2(saph)_2q_2$ as a novel host material for red-dopant light-emitting diodes. The large improvement of our devices is not only due to the excellent energy match between the host $Ga_2(saph)_2q_2$ and the guest but also to the superior properties of $Ga_2(saph)_2q_2$ as a host. DCJTB is known to be excited mainly by energy transfer from the host, which is a competitive process against the thermal deactivation of the excited host material. It is therefore reasonable to assume that the host $Ga_2(saph)_2q_2$, having much higher PL quantum yield, provides higher EL efficiency because of its higher energy transfer efficiency.[10] Moreover, the higher T_g and much better thermal stability are also helpful to improve the durability of the devices. Figure 7 shows the preliminary study on the operational stability of the above $Ga_2(saph)_2q_2$- and Alq_3-doped OLEDs. Under the same conditions (without encapsulation), the $Ga_2(saph)_2q_2$-doped device exhibited a much longer lifetime than the Alq_3 device. The initial brightness was 1000 cd/m^2. After 10 h of operation, the light output of $Ga_2(saph)_2q_2$-doped devices decreased to 880 cd/m^2 at 17 mA of constant current. The voltage shifts slightly from 7.5

to 7.7 V. As a whole, the decay process was slower. However, the Alq_3-doped devices decayed more rapidly and dropped to 720 cd/m^2 after 10 h of operation. Also, the voltage showed a large shift from 11.3 to 11.8 V. Further study on the durability of the $Ga_2(saph)_2q_2$ devices is still in progress.

Summary

In conclusion, we have demonstrated a binuclear gallium complex with mixed ligands based on tridentate ligands of a Schiff base, $Ga_2(saph)_2q_2$, which exhibits a combination of both intramolecular and intermolecular interactions of the q ligands, which is different from Gaq_3. In addition, this binuclear complex possesses much higher luminescent efficiency and better thermal stability than the typical tris(8-hydroxyquinolinolate)metal complexes with central metal ions of Al^{3+} or Ga^{3+}. These distinguishing properties further confirm that $Ga_2(saph)_2q_2$ has great potential as an active material for OLEDs.

We have also recently synthesized a series of binuclear aluminum complexes with a β-diketone and the tridentate saph ligand, which show extremely high photoluminescence efficiency as compared to Alq_3. The preliminary studies make it clear that the effective combination of different mixed ligands can result in binuclear complexes with tunable luminescent efficiency and carrier mobility. This would be a potential path for the design of organic metal complexes used in OLEDs. The results of these studies will be reported in future publications.

Acknowledgment. This work is financially supported by the National Natural Science Foundation of China (No. 90101029). We thank Associate Professor Ruji Wang for X-ray diffraction measurements and analysis.

Supporting Information Available: X-ray crystallographic data in CIF format for the structure determination of $Ga_2(saph)_2q_2$, CCDC 195495. This material is available free of charge via the Internet at http://pubs.acs.org.

IC049603S